

This is the accepted manuscript made available via CHORUS. The article has been published as:

# X-ray natural dichroism and chiral order in underdoped cuprates

M. R. Norman

Phys. Rev. B **87**, 180506 — Published 23 May 2013

DOI: [10.1103/PhysRevB.87.180506](https://doi.org/10.1103/PhysRevB.87.180506)

# X-ray natural dichroism and chiral order in underdoped cuprates

M. R. Norman<sup>1</sup>

<sup>1</sup>*Materials Science Division, Argonne National Laboratory, Argonne, IL 60439, USA*

(Dated: May 14, 2013)

The origin of the Kerr rotation observed in the pseudogap phase of cuprates has been the subject of much speculation. Recently, it has been proposed that this rotation might be due to chiral charge order. Here, I investigate whether such order can be observed by x-ray natural circular dichroism (XNCD). Several types of charge order were considered, and they can give rise to an XNCD signal depending on the stacking of the order along the c-axis.

PACS numbers: 78.70.Dm, 75.25.+z, 74.72.Hs

Since its observation over twenty years ago, the nature of the pseudogap phase in underdoped cuprates has been a subject of much debate<sup>1,2</sup>. Time reversal symmetry breaking was proposed by Varma<sup>3</sup>, and based on this prediction, angle resolved photoemission (ARPES) experiments were done by Kaminski *et al.*<sup>4</sup> on underdoped Bi<sub>2</sub>Sr<sub>2</sub>CaCu<sub>2</sub>O<sub>8+δ</sub> (Bi2212) that did indeed observe a dichroism signal by using circularly polarized light. Their signal was consistent with an order parameter like temperature evolution that set in below the pseudogap temperature T\*. These results, though, have yet to be confirmed by other groups<sup>5</sup>. Moreover, even if confirmed, such a signal could instead be due to chiral order or certain types of structural distortions rather than time reversal breaking. On the other hand, subsequent elastic neutron scattering experiments did observe time reversal breaking in underdoped YBa<sub>2</sub>Cu<sub>3</sub>O<sub>6+x</sub> (YBCO)<sup>6</sup> that sets in below T\*. This has now been seen in a variety of cuprates<sup>7</sup>. Interestingly, this symmetry breaking has not been seen by  $\mu$ SR<sup>8</sup>, implying that the observed order is actually fluctuating in nature.

After the neutron results, a novel Sagnac interferometry experiment was done by Kapitulnik's group<sup>9</sup> that observed a Kerr rotation that sets in at a temperature below that where the elastic magnetic signal is first seen by neutrons. In Bi<sub>2</sub>Sr<sub>2</sub>CuO<sub>6+δ</sub> (Bi2201), a similar signal was seen that set in at the same temperature ARPES measurements saw an energy gap develop<sup>10</sup>. Originally, it was suggested that this signal was a signature of a tiny ferromagnetic moment, but as Orenstein has pointed out<sup>11</sup>, a Kerr rotation was seen in the antiferromagnet Cr<sub>2</sub>O<sub>3</sub> where a structural distortion accompanies the magnetic order<sup>12</sup>. This occurs since although  $\langle P \rangle$  and  $\langle M \rangle$  vanish because of the staggered order (where  $P$  is the polarization and  $M$  the magnetization),  $\langle P \cdot M \rangle$  is non-zero. That is, the structural distortion flips sign with the moment, and so the scalar product is invariant to the staggering. A different magneto-chiral phase has recently been advocated by Varma and collaborators based on orbital currents to explain the Kerr effect in the cuprates<sup>13</sup>. But the idea of chiral charge order has also been proposed<sup>14,15</sup>. One motivation for the latter proposal is that the onset of the Kerr rotation in YBCO does not occur at T\*, but rather at a lower temperature

where charge order has been seen to develop by x-ray scattering<sup>16,17</sup>.

To further explore this, it would be useful to identify other probes that could detect such chiral order. XNCD is a natural one to propose<sup>18</sup>. This is the difference in absorption of left and right circularly polarized light from time even processes (as opposed to magnetic circular dichroism which comes from time odd processes). It is sensitive to inversion symmetry breaking, and as it is site specific, it can be used to gain information on the spatial nature of the order. Interestingly, an XNCD signal was seen at the Cu K edge in Bi2212<sup>19</sup> that has an order parameter like evolution with temperature that matched the ARPES dichroism signal. Though many space group refinements of Bi2212 break inversion symmetry, because of the presence of glide planes (mirror planes plus translations), the XNCD signal due to the crystal structure is zero when the light is directed along the c-axis<sup>20</sup> as in the experiment. A lower symmetry than simply the crystal structure would be required to generate an XNCD signal, and chiral order could indeed satisfy this condition.

In the present paper, I investigate whether such chiral order could be the source of an XNCD signal, and find that if the order is such as to violate the two glide planes present in Bi2212 (one perpendicular to the CuO<sub>2</sub> planes, the other parallel), then an XNCD signal does occur.

I start with a discussion of the Bi2212 space group. The basic unit cell is face centered orthorhombic. For purposes here, the superstructure modulation observed in Bi2212 is ignored, since this involves a translation operation that is not relevant to the symmetry considerations allowing for XNCD. In our previous study<sup>20</sup>, several space group refinements were considered, but for the purposes of this paper, two will be studied. The first one (Bb2b) of Gladyshevskii and Flükiger<sup>21</sup> is non-centrosymmetric, the second one (Bbmb) of Miles *et al.*<sup>22</sup> is centrosymmetric. All refinements have in common the existence of two glide planes (with the glides along the supermodulation b-axis), one perpendicular to the a-axis which runs through the planar oxygen ions<sup>23</sup>, the other perpendicular to the c-axis (midway between successive CuO<sub>2</sub> bilayer units, which is also midway between the two BiO planes). One can easily see that any given order must violate both glide planes in order to give a non-zero

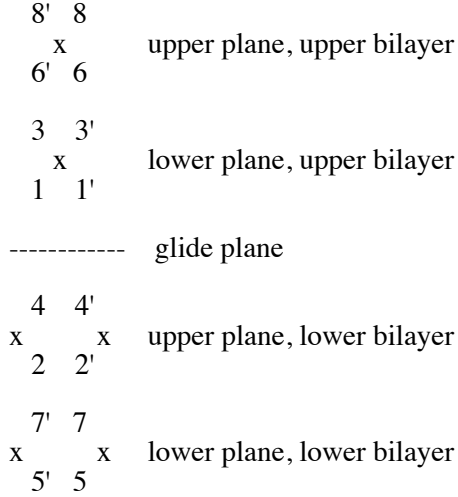


FIG. 1: Oxygen sites in the four  $\text{CuO}_2$  planes of the unit cell of Bi2212 (shown are four oxygens per plane). The numbers refer to the space group operations in the text, with the two different planar oxygen sites shown as unprimed and primed. x denotes the location of the coppers. The a-axis runs along 1-1', the b-axis along 1-3, with a glide plane along 1-3 as well. The other glide plane ( $\perp c$ ) is shown as the dashed line.

signal, since XNCD involves a sum over all the atoms in the crystal associated with the x-ray edge studied. That is, in the presence of a mirror operation, the XNCD signal from two atoms related by the mirror cancel.

XNCD originates from interference between dipole (E1) and quadrupole (E2) contributions to x-ray absorption<sup>18</sup>. This requires inversion symmetry to be broken. This contribution is a time even pseudo-deviator (parity odd second rank tensor)<sup>24</sup>, which for most (but not all) symmetries would give rise to optical dichroism as well (a pseudo-scalar)<sup>25</sup>. There can be a contribution to XNCD as well from interference between electric (E1) and magnetic (M1) dipoles, but this contribution is very small, which was verified in the present case by numerical simulations.

Numerical results are generated using the FDMNES program<sup>26,27</sup>. The simulations were done using local density atomic potentials (Hedin-Lunqvist exchange-correlation function) in a muffin tin approximation that considers multiple scattering of the photoelectron around the absorbing site<sup>28,29</sup>. The cluster radius is limited by the photoelectron escape depth<sup>30</sup>. Here, fixed cluster radii of 3.1Å and 4.9Å are considered as in Ref. 20, but in one case, larger clusters of radii 5.5Å and 6.5Å were studied. For all calculations shown, the incident light is along the c-axis.

To proceed, discussing symmetries of the  $\text{CuO}_2$  planes for Bi2212 is in order (Fig. 1). There are two different planar oxygen sites, each of which forms rows along the b-axis, with the different rows alternating as one moves along the a-axis. Associated with this is a glide plane or-

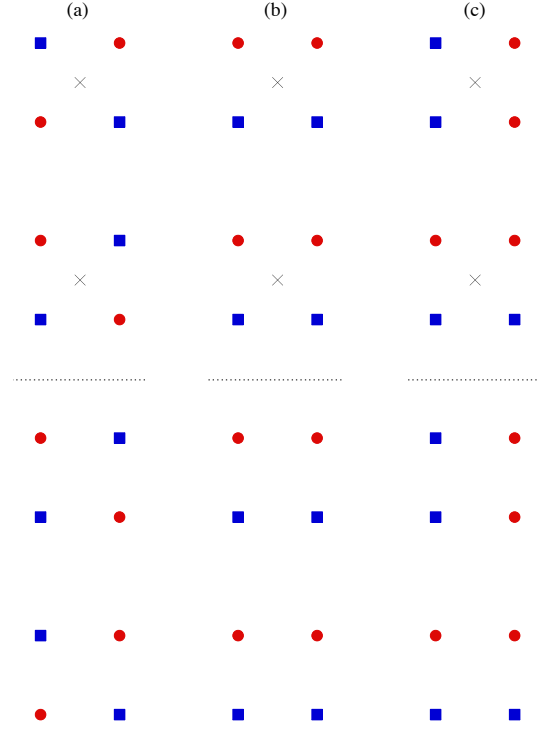


FIG. 2: (Color online) Three charge patterns considered in the text - (a) pattern 1, (b) pattern 2, and (c) pattern 3. Circles and squares are oxygen ions, crosses are coppers. Positions of the ions are as in Fig. 1. In the calculations, squares have a charge excess of 0.1, circles a charge deficiency of 0.1.

thogonal to the a-axis. There are also four  $\text{CuO}_2$  planes per unit cell, composing an upper bilayer and a lower bilayer, with another glide plane in between the two bilayers. The two oxygen rows are interchanged as one moves from each layer to the next, with the upper plane of the upper bilayer and the lower plane of the lower bilayer having the same pattern, and the other two planes staggered relative to this by half a lattice constant along the a-axis. Note that as a consequence of these two different planar oxygen sites, even in centrosymmetric refinements of Bi2212, inversion symmetry is locally broken about the copper sites. As for the copper atoms, they stagger differently, translating along the a-axis by half a lattice constant as one goes from one bilayer to the next. This can be understood from the eight space group operations, which are (1) the identity, (2) two-fold rotation  $(-x, y, -z)$ , (3) first glide  $(-x, y+1/2, z)$ , (4) second glide  $(x, y+1/2, -z)$ , and then (5-8) the above operations followed by the face centering translation  $(1/2, 0, 1/2)$ . These operations are used to label the oxygen ions in Fig. 1.

I will now consider charge ordering patterns on the oxygens that do not break translational symmetry, since this is what the neutron data indicate<sup>6</sup>, and as mentioned above, the translational part of any order is not relevant for the symmetry considerations allowing for an XNCD signal. Fig. 2a shows a pattern that is the charge ana-

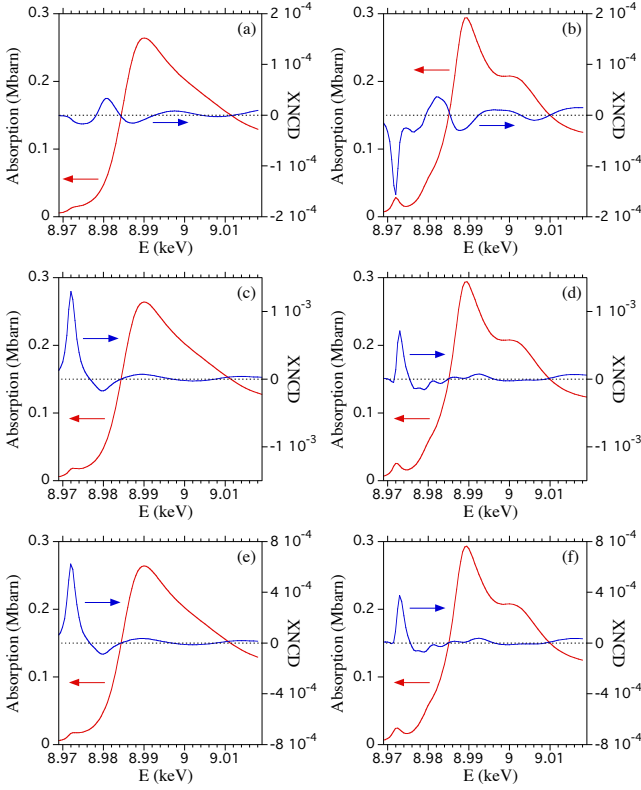


FIG. 3: (Color online) XNCD for the various charge patterns described in the text at the Cu K edge in Bi2212 (with  $k$  along the  $c$ -axis) for the crystal refinement of Ref. 21. Also shown is the absorption signal itself. The left column is for a cluster radius of 3.1 Å, the right one for 4.9 Å. The top row is for pattern 1, the middle row for pattern 2, and the bottom row for pattern 3. Note the differing scales on the right y-axis for each row.

logue of the oxygen spin pattern that was considered in Ref. 6 as an alternate to orbital currents, referred to here as pattern 1. Note that this pattern breaks the first glide. Another pattern, referred to as pattern 2, flips the charges in the second row of oxygen ions (Fig. 2b). This pattern also violates the first glide. To violate the second glide, these two patterns must have the correct staggering along the  $c$ -axis. For pattern 1, the staggering is  $(-, +, +, -)$  where the order refers to the plane sequence (upper plane, upper bilayer; lower plane, upper bilayer; upper plane, lower bilayer; lower plane, lower bilayer) as in Fig. 1, with the sign referring to that of the oxygen site in the lower left corner of each plane ( $6', 1, 2, 5'$ ). All other stackings with an even number of  $+$  and  $-$  signs give a vanishing signal. For pattern 2, a non-zero signal under the same condition of an even number of  $+$  and  $-$  signs requires that all planes are in phase  $(+, +, +, +)$ . In both cases, the space group reduces to B121 with four operations: the identity, two-fold rotation  $(-x, y, -z)$ , and the face centering translation  $(1/2, 0, 1/2)$  of these two.

Next, a true chiral pattern is considered based on the suggestion of Ref. 14. This pattern is the same as in

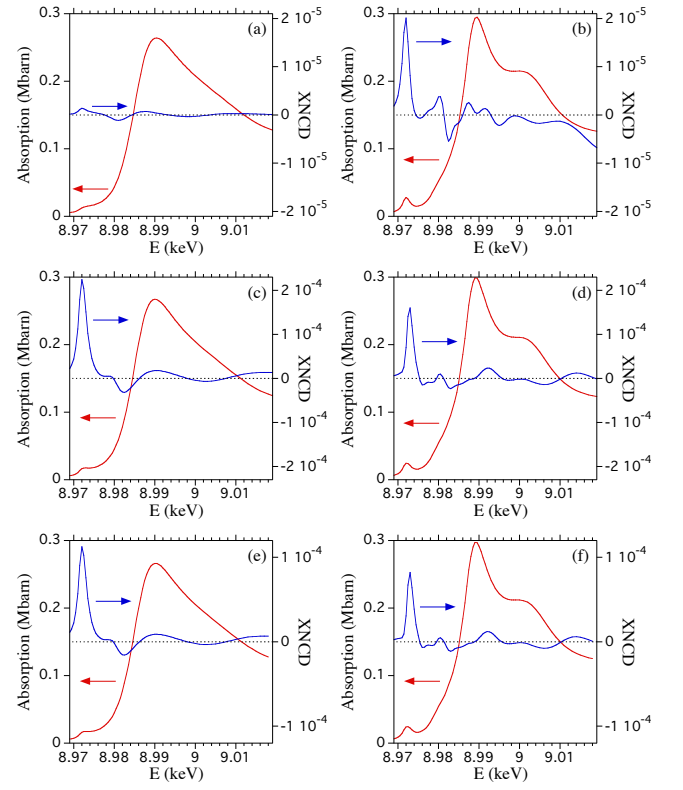


FIG. 4: (Color online) XNCD for the various charge patterns described in the text at the Cu K edge in Bi2212 (with  $k$  along the  $c$ -axis) for the crystal refinement of Ref. 22. Same notation as in Fig. 3.

Fig. 2b, except it is rotated around the center of the four oxygen sites in each plane as one goes from plane to plane, with a rotation sequence of  $(-90^\circ, 0^\circ, 90^\circ, 180^\circ)$ . This pattern, though, preserves the symmetry operation  $(-x+1/2, y+1/2, z+1/2)$  and thus has a vanishing XNCD signal. An alternate pattern presented in Ref. 15 has the rotation sequence  $(-90^\circ, 0^\circ, -90^\circ, 0^\circ)$ . This pattern (Fig. 2c), denoted as pattern 3, breaks all symmetries (P1 space group), allowing for XNCD.

Fig. 3 shows the calculated XNCD signal at the Cu K edge for the three patterns with a cluster radius of 3.1 Å (a copper and its five surrounding oxygen ions) in the left column, and a cluster radius of 4.9 Å (which contains 37 atoms) in the right column. Spin-orbit was included, but this only had a modest effect. A charge imbalance of  $\pm 0.1 e^-$  was assumed on the oxygen sites. Note that flipping the charge pattern flips the dichroism signal. Complex energy profiles are found. They differ between the various charge patterns, and are sensitive to the cluster radius. Note that the dichroism in pattern 3 is half that of pattern 2. This can be understood from the symmetry of the two patterns shown in Fig. 2. The magnitude of the dichroism is significant, with values up to  $4 \times 10^{-3}$  of the absorption maximum, which is not only larger than that claimed in Ref. 19, but well within the range of detection of modern x-ray sources. The largest signal typically is

seen at the pre-edge peak at 8.972 keV, expected since this corresponds to  $1s - 3d$  excitations (as opposed to the edge itself, which corresponds to  $1s - 4p$  excitations). This is in contrast to the experimental result, which is simply a positive peak at 8.99 keV followed by a negative peak at 8.998 keV. As discussed in our earlier work<sup>20</sup>, the observed signal seems most consistent with a small energy shift between left and right circularly polarized light, rather than intrinsic dichroism. Regardless, the XNCD energy profile calculated here is very sensitive to the nature of the charge order, thus providing a unique fingerprint for this order.

In Fig. 4, results are shown for the centrosymmetric refinement of Miles *et al.*<sup>22</sup>. Generally, the dichroism is about an order of magnitude smaller, not surprising since this refinement preserves inversion symmetry. Larger cluster radii were also run for pattern 2 (5.5Å and 6.5Å). The 5.5Å result was similar to the 4.9Å one, whereas the 6.5Å one had a pre-edge XNCD signal which was partially suppressed. Still, the XNCD signal is generally large enough that it should be detectable if present.

In summary, I find that XNCD should be an exquisite probe of chiral order in cuprates, assuming that the order is such to allow a non-zero XNCD signal. Each charge pattern calculated has a unique energy profile that should be detectable at modern x-ray sources. In fact, a variety of potential x-ray measurements could be done that would allow for a thorough interrogation of such order, including its potential magneto-chiral nature<sup>24,31</sup>, and it would be quite interesting if such experiments were attempted on a variety of cuprates.

Work at Argonne is supported by Basic Energy Sciences, Office of Science, U.S. Dept. of Energy, under Contract No. DE-AC02-06CH11357. The author would like to thank Sergio Di Matteo for many helpful discussions.

- <sup>1</sup> T. Timusk and B. Statt, Rep. Prog. Phys. **62**, 61 (1999).
- <sup>2</sup> M. R. Norman, D. Pines and C. Kallin, Adv. Phys. **54**, 715 (2005).
- <sup>3</sup> C. M. Varma, Phys. Rev. B **61**, R3804 (2000); M. E. Simon and C. M. Varma, Phys. Rev. Lett. **89**, 247003 (2002).
- <sup>4</sup> A. Kaminski, S. Rosenkranz, H. Fretwell, J. C. Cam-puzano, Z. Li, H. Raffy, W. G. Cullen, H. You, C. G. Olson, C. M. Varma and H. Hoehst, Nature **416**, 610 (2002).
- <sup>5</sup> S. V. Borisenko, A. A. Kordyuk, A. Koitzsch, T. K. Kim, K. A. Nenkov, M. Knupfer, J. Fink, C. Grazioli, S. Turchini and H. Berger, Phys. Rev. Lett. **92**, 207001 (2004).
- <sup>6</sup> B. Fauqué, Y. Sidis, V. Hinkov, S. Pailhes, C. T. Lin, X. Chaud and P. Bourges, Phys. Rev. Lett. **96**, 197001 (2006).
- <sup>7</sup> P. Bourges and Y. Sidis, Comptes Rendus Physique **12**, 461 (2011).
- <sup>8</sup> G. J. MacDougall, A. A. Aczel, J. P. Carlo, T. Ito, J. Rodriguez, P. L. Russo, Y. J. Uemura, S. Wakimoto and G. M. Luke, Phys. Rev. Lett. **101**, 017001 (2008).
- <sup>9</sup> J. Xia, E. Schemm, G. Deutscher, S. A. Kivelson, D. A. Bonn, W. N. Hardy, R. Liang, W. Siemons, G. Koster, M. M. Fejer and A. Kapitulnik, Phys. Rev. Lett. **100**, 127002 (2008).
- <sup>10</sup> R.-H. He, M. Hashimoto, H. Karapetyan, J. D. Koralek, J. P. Hinton, J. P. Testaud, V. Nathan, Y. Yoshida, H. Yao, K. Tanaka, W. Meevasana, R. G. Moore, D. H. Lu, S.-K. Mo, M. Ishikado, H. Eisaki, Z. Hussain, T. P. Devereaux, S. A. Kivelson, J. Orenstein, A. Kapitulnik and Z.-X. Shen, Science **331**, 1579 (2011).
- <sup>11</sup> J. Orenstein, Phys. Rev. Lett. **107**, 067002 (2011).
- <sup>12</sup> B. B. Krichevtsov, V. V. Pavlov, R. V. Pisarev and V. N. Gridnev, J. Phys.: Condens. Matter **5**, 8233 (1993).
- <sup>13</sup> V. Aji, Y. He and C. M. Varma, arXiv:1211.1391
- <sup>14</sup> P. Hosur, A. Kapitulnik, S. A. Kivelson, J. Orenstein and S. Raghu, Phys. Rev. B **87**, 115116 (2013).
- <sup>15</sup> J. Orenstein and J. E. Moore, Phys. Rev. B **87**, 165110 (2013).
- <sup>16</sup> G. Ghiringhelli, M. Le Tacon, M. Minola, S. Blanco-Canosa, C. Mazzoli, N. B. Brookes, G. M. De Luca, A. Frano, D. G. Hawthorn, F. He, T. Loew, M. Moretti Sala, D. C. Peets, M. Salluzzo, E. Schierle, R. Sutarto, G. A. Sawatzky, E. Weschke, B. Keimer and L. Braicovich, Science **337**, 821 (2012).
- <sup>17</sup> J. Chang, E. Blackburn, A. T. Holmes, N. B. Christensen, J. Larsen, J. Mesot, R. Liang, D. A. Bonn, W. N. Hardy, A. Watenphul, M. v. Zimmermann, E. M. Forgan and S. M. Hayden, Nature Phys. **8**, 871 (2012).
- <sup>18</sup> L. Alagna, T. Prosperi, S. Turchini, J. Goulon, A. Rogalev, C. Goulon-Ginet, C. R. Natoli, R. D. Peacock and B. Stewart, Phys. Rev. Lett. **80**, 4799 (1998).
- <sup>19</sup> M. Kubota, K. Ono, Y. Oohara and H. Eisaki, J. Phys. Soc. Japan **75**, 053706 (2006).
- <sup>20</sup> S. Di Matteo and M. R. Norman, Phys. Rev. B **76**, 014510 (2007).
- <sup>21</sup> R. E. Gladyshevskii and R. Flükiger, Acta Cryst. **B52**, 38 (1996).
- <sup>22</sup> P. A. Miles, S. J. Kennedy, G. J. McIntyre, G. D. Gu, G. J. Russell and N. Koshizuka, Physica C **294**, 275 (1998).
- <sup>23</sup> For non-centrosymmetric refinements, the oxygen ions are slightly displaced off the glide plane.
- <sup>24</sup> J. Goulon, A. Rogalev, F. Wilhelm, C. Goulon-Ginet, P. Carra, I. Marri and Ch. Brouder, J. Exp. Theor. Phys. **97**, 402 (2003).
- <sup>25</sup> J. Jerphagnon and D. S. Chemla, J. Chem. Phys. **65**, 1522 (1976).
- <sup>26</sup> Y. Joly, Phys. Rev. B **63**, 125120 (2001). The FDMNES program can be downloaded at <http://neel.cnrs.fr/spip.php?rubrique1007>
- <sup>27</sup> Y. Joly, O. Bunau, J. E. Lorenzo, R. M. Galera, S. Grenier and B. Thompson, J. Phys.: Conf. Ser. **190**, 012007 (2009).
- <sup>28</sup> C. R. Natoli, Ch. Brouder, Ph. Saintavit, J. Goulon, Ch. Goulon-Ginet and A. Rogalev, Eur. Phys. J. B **4**, 1 (1998).
- <sup>29</sup> When constructing the potentials, it is assumed that the coppers are in a  $d^9s^2$  configuration and the oxygens in a  $p^{4\pm0.1}s^2$  configuration.
- <sup>30</sup> The results presented involve a convolution of the calculated spectrum with both a core hole (1.89 eV) and a photoelectron lifetime, with the latter having a strong energy dependence (at high energies, 15 eV, with a midpoint value at 30 eV above the Fermi energy). A Fermi energy (i.e., a core level shift) of -7.4 eV was assumed. Calculations were also done with a Fermi energy determined by the code, which led to only minor differences in the pre-edge region.
- <sup>31</sup> S. Di Matteo and C. M. Varma, Phys. Rev. B **67**, 134502 (2003).